PCCP

Chemical process of hydrogen and formic acid on a Pd-deposited Cu(111) surface studied by high-resolution X-ray photoelectron spectroscopy and density functional theory calculations

Journal:	*Physical Chemistry Chemical Physics*
Manuscript ID	CP-ART-10-2024-003942.R1
Article Type:	Paper
Date Submitted by the Author:	08-Dec-2024

Complete List of Authors:	Osada, Wataru; The University of Tokyo, The Institute for Solid State Physics Hasegawa, Masahiro; The University of Tokyo, The Institute for Solid State Physics Shiozawa, Yuichiro; Yamanashi Prefectural Industrial Technology Center Mukai, Kozo; The University of Tokyo, The Institute for Solid State Physics Yoshimoto, Shinya; The University of Tokyo, The Institute for Solid State Physics Tanaka, Shunsuke; The University of Tokyo, The Institute for Solid State Physics Kawamura, Mitsuaki; RIKEN, Center for Emergent Matter Scienc Ozaki, Taisuke; The University of Tokyo, The Institute for Solid State Physics Yoshinobu, J.; The University of Tokyo, The Institute for Solid State Physics

ARTICLE

Chemical process of hydrogen and formic acid on a Pd-deposited Cu(111) surface studied by high-resolution X-ray photoelectron spectroscopy and density functional theory calculations

Received 00th January 20xx,
Accepted 00th January 20xx

DOI: 10.1039/x0xx00000x

Wataru Osada,†[a] Masahiro Hasegawa,†[a] Yuichiro Shiozawa,†[a] Kozo Mukai,[a] Shinya Yoshimoto,[a] Shunsuke Tanaka,[a] Mitsuaki Kawamura,[b] Taisuke Ozaki [a] and Jun Yoshinobu *[a]

Formic acid (HCOOH) is one of the essential molecules for CO_2 utilization including methanol synthesis and hydrogen carriers. In this study, we have investigated the chemical processes of hydrogen and HCOOH on a dilute-alloy Pd-Cu(111) surface using high-resolution X-ray photoelectron spectroscopy (HR-XPS) and density functional theory (DFT) calculations. The present Pd-Cu(111) surface was prepared at 500 K, and the observed core-level shifts of Pd $3d_{5/2}$ indicate that Pd atoms were located at the surface and subsurface sites: 335.3 eV at the surface and 335.6 eV at subsurface sites, respectively. The coverage of surface Pd atoms was estimated to be 0.05 ML, indicating that the present Pd-Cu(111) surface acted as a single atom alloy catalyst. The observed C 1s and O 1s XPS spectra indicate that the surface chemistry of HCOOH on the present Pd-Cu(111) surface is almost equivalent to a bare Cu(111) surface; HCOOH is dissociated into monodentate formate and atomic hydrogen at 150-160 K, followed by conversion to bidentate formate species at 300 K, and finally it is decomposed and desorbed as CO_2 + ½ H_2 at ~450 K. The conversion ratio of adsorbed HCOOH to bidentate formate species on Pd-Cu(111) was 12 %, almost the same as that on Cu(111). That monodentate formate species and atomic hydrogen aggregate around the Pd atom is supported by the observed core-level shift of Pd $3d_{5/2}$ and systematic DFT calculations . The present DFT calculations also show that formate species are preferably adsorbed on the Cu site; thus, the Pd site is unoccupied by formate species at this stage. This implies that the present single atom alloy catalyst Pd-Cu(111) has an advantage during CO_2 hydrogenation, where the Pd site can act as the H_2 dissociation site without poisoning by formate intermediate species.

I. Introduction

The hydrogenation of carbon dioxide (CO_2) is one of the most demanded approaches to reducing CO_2, recycling carbon resources and achieving a carbon-neutral society.[1,2] Many chemical products/feedstocks can be produced by CO_2 hydrogenation: methanol, formic acid, formaldehyde, dimethyl ether, hydrocarbons, and so on.[3] In these materials, methanol has attracted great attention because of its versatility as a chemical feedstock in the chemical industry.[4,5] In the current chemical industry, Cu-ZnO catalysts have been used in methanol synthesis from syngas (mixture of CO and H_2),[3,4] and these Cu-based catalysts also show activity in CO_2 hydrogenation.[4,5] Therefore, many works have been reported on methanol synthesis by CO_2 hydrogenation on various Cu-based catalysts.[1–8] Various reaction mechanisms from CO_2 to methanol have been proposed in these studies; the theory of a pathway through formate intermediate has been widely supported.[1,3]

Detailed knowledge of formate species adsorbed on Cu surfaces, including the adsorption structure and processes of decomposition and formation, has been accumulated by experimental[9–29] and theoretical studies.[18,20,30–35] One of the processes forming adsorbed formate species is the dissociative adsorption of formic acid (HCOOH). In methanol synthesis, HCOOH has also been proposed as an intermediate product.[3,30,36] Furthermore, the hydrogen energy carrier system using HCOOH has been proposed, where HCOOH is reversely converted to CO_2 and H_2 (HCOOH ⇄ CO_2 + H_2).[37] Thus, understanding the surface chemistry of HCOOH on Cu surfaces is an important issue in the context of CO_2 utilization.

Recently, we have systematically studied the surface processes of HCOOH on flat and vicinal Cu surfaces using several surface science techniques and theoretical calculations.[15,19,20,22] These studies have elucidated the importance of the step sites on the Cu surface[19,22] and hydrogen bonding[15,20,22] on the surface chemistry of HCOOH on Cu surfaces. We have also investigated formic acid and formate species on Zn-decorated Cu surfaces and concluded that the formate species were stabilized on the steps decorated by Zn.[19] This conclusion has been reported by other previous studies.[17,30]

[a] The Institute for Solid State Physics, The University of Tokyo, 5-1-5 Kashiwanoha, Kashiwa, Chiba 277-8581, Japan. E-mail: junyoshi@issp.u-tokyo.ac.jp
[b] Center for Emergent Matter Science, RIKEN, 2-1 Hirosawa, Wako, Saitama 351-0198, Japan
† Present address: National Metrology Institute of Japan, National Institute for Advanced Industrial Science and Technology, 1-1-1 Umezono, Tsukuba, Ibaraki 305-8563 (W. O.); National Consumer Affairs Center of JAPAN, 3-1-1 Yaei, Chuo-ku, Sagamihara-shi, Kanagawa 400-0055, Japan (M. H.); Yamanashi prefectural Industrial Technology Center, 2094 Otsu-machi, Kofu, Yamanashi 400-0055, Japan (Y.S.).

In this paper, we focused on the effect of dilute Pd atoms on a Cu surface on the surface process of HCOOH because a Pd-Cu alloy surface can be expected to be a superior catalyst for CO_2 hydrogenation into methanol.[38–42] We prepared the dilute-alloy model catalyst Pd-Cu(111), where the present surface acted as a single atom alloy catalyst (SAAC),[43] and investigated the chemical process of HCOOH on the surface using high-resolution X-ray photoelectron spectroscopy (HR-XPS). In addition, the hydrogen-exposed Pd-Cu(111) surface was investigated, because the Pd atoms embedded in the Cu(111) show excellent activity for hydrogen dissociation.[44–47] Further, we performed density functional theory (DFT) calculations to elucidate the adsorbed states and the chemical shift in the HR-XPS spectra. The present experimental and theoretical results provide a quantitative understanding of the surface chemistry of HCOOH on a dilute-alloy Pd-Cu(111) surface, including the conversion ratio into formate species, the adsorption structure near the Pd site, and the Pd $3d_{5/2}$ core-level shifts. In particular, the present results show that the Pd site of Pd-Cu(111) is not occupied by formate species. This suggests that the present Pd-Cu SAAC has an advantage in methanol synthesis via CO_2 hydrogenation, where the single atom Pd site can act as the H_2 dissociation site without poisoning by intermediate species such as formate species.

II. Experimental

A clean Cu(111) surface was prepared by repeated cycles of Ne^+ sputtering and annealing at 673 K. The temperature of the sample was measured by a K-type thermocouple attached to the side of a Cu crystal by a Ta foil. The clean, well-defined Cu(111) surface was checked by XPS and low energy electron diffraction. A Pd-Cu dilute-alloy surface was prepared by vapor deposition of Pd on Cu(111) at 500 K using a homemade Pd wire source.[45] According to the previous studies, the optimal temperature to prepare the Pd-Cu(111) SAA surface is 380 K or below, and the deposition at higher temperatures could lead migration of Pd atoms into the subsurface/bulk regions.[45,46,48] In this study, heating above 450 K is necessary to investigate the chemical process of HCOOH and formate species on the Cu-based model catalysts.[19,49] Therefore, in order to discuss the electronic states of surface Pd only caused by the interaction with HCOOH, formate and hydrogen ad-species, we chose the deposition temperature of 500 K. HR-XPS measurements were perform-ed using a UHV chamber (base pressure < 2×10^{-10} Torr) at the soft X-ray undulator beamline (BL-13B) of the Photon Factory in Tsukuba, Japan.[50] All of the HR-XPS spectra shown in this paper were measured using a hemispherical electron analyser (SPECS, Phoibos 100) at a normal emission angle with a pass energy of 6 eV. The incidence angle of the X-ray was 45° with respect to the surface normal. C 1s and O 1s core level regions were measured at a photon energy ($h\nu$) of 680 eV, and Pd $3d_{5/2}$ and Cu 3p core levels were measured at $h\nu$ = 490 eV. The C 1s and Pd $3d_{5/2}$ spectra were deconvoluted using a Voigt function and a Shirley background.

Gaseous hydrogen was introduced to the prepared Pd-Cu(111) surface through a variable leak valve. Formic acid (HCOOH, Wako Chemicals, >98.0 % purity) vapor was introduced into the UHV chamber using a pulse valve. Water and other impurities in the HCOOH were removed by copper sulphate anhydride and several cycles of freeze-pump-thaw. The coverage of HCOOH was estimated from the C 1s peak. The C 1s spectrum for the first layer of cyclohexane on Cu(111) was used as a reference.[19,51] In the case of the deposited Pd, the coverage was estimated from the peak area ratio of Pd $3d_{5/2}$/Cu 3p, where we calibrated the observed peak areas with several factors including the differential photoionized cross sections,[52,53] the depth distribution function,[54] and the transmission function at the present analyser. The transmission function of the electron analyser was evaluated by the method in the literature.[55,56]

For DFT calculations, OpenMX code was used.[57,58] The exchange-correlation effect was represented by generalized gradient approximation with the Perdew-Burke-Ernzerhof (GGA-PBE) method.[59] To take into account van der Waals interaction, the dispersion-corrected DFT (DFT-D3) approach was applied.[60,61] A slab model for the representation of Pd/Cu(111) consisted of a (4×4) unit cell with a four-atomic layer and ~15 Å vacuum layer. In geometry optimization, the Cu atoms in the bottom two layers were fixed in their bulk position. The adsorption energy, ΔH_{ad}, is defined as:

$$\Delta H_{ad} = E_{adsorbate/substrate} - E_{gas} - E_{substrate}$$

where $E_{adsorbate/substrate}$, E_{gas}, and $E_{substrate}$ are the total energies of the adsorbate bound surface, the gaseous molecules, and the clean surface, respectively. For core level excitation, fully relativistic pseudopotentials and pseudoatomic orbitals were used.[62,63] All of the pseudopotentials and basis functionals used in this paper are provided on the OpenMX website.[62,64]

III. Results and discussion

A: HR-XPS measurements on a clean and H_2-exposed Pd-Cu(111) surface

First, in order to characterize the present prepared Pd-Cu(111) surface, we investigated clean and hydrogen-exposed Pd-Cu(111) surfaces using HR-XPS. A Pd-Cu(111) surface was prepared following the procedure described in section II. Figure 1(a) shows the Pd $3d_{5/2}$ spectra of the Pd-Cu(111) surface as a function of the experimental processes from (A) to (E). Spectrum (A) in Fig. 1(a) was measured on the as-deposited Pd-Cu(111) surface at room temperature and consists of two components at 335.3 eV and 335.6 eV. Previously, we reported the HR-XPS spectra for a Pd-Cu(111) surface prepared at 380 K, where only one component was observed at 335.3 eV.[47] It has been reported that some of the deposited Pd atoms migrate into the subsurface and/or bulk of the Cu crystal by preparation at higher temperatures (>435 K).[46,48,65] Since the present sample surface was prepared at 500 K, some Pd atoms could migrate to the subsurface and/or bulk sites. Therefore, the component at 335.6 eV can be tentatively assigned to the Pd atoms at the subsurface. This assignment is further supported by experimental and theoretical investigations, which will be discussed later.

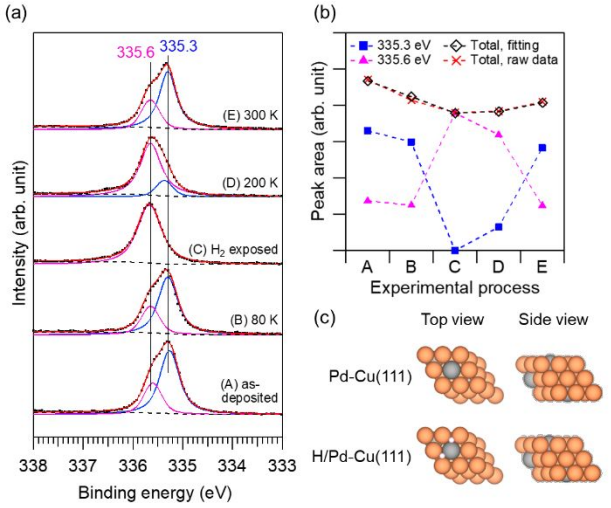

Fig. 1 (a) Pd $3d_{5/2}$ XPS spectra (A) on a clean Pd-Cu(111) surface at room temperature, (B) at 80 K, and after (C) 200 L H_2 exposure, (D) after heating to 200 K, and (E) after heating to 300 K. Spectra (C) to (E) were measured at 80 K. The coverage of the surface Pd was estimated to be ~0.1 ML. The spectra were measured with a photon energy of 490 eV. Peak fitting was conducted using Voigt peaks with a Shirley background. (b) Changes in the peak areas for total spectra and each component. (c) Model structures of the clean (upper) and hydrogen-adsorbed Pd-Cu(111) (lower). Pd atoms are placed not only at the surface but also at the subsurface. The orange, grey, and white spheres represent Cu, Pd, and H atoms, respectively.

Spectra (B)-(E) in Fig. 1(a) are a series of the hydrogen adsorption and desorption experiments from 80 K to 300 K. Spectrum (B) was measured after cooling to 80 K, which is almost the same as spectrum (A). When the surface was exposed to 200 L H_2, the component at 335.3 eV disappeared, and only one peak was observed at 335.6 eV (spectrum (C)). Spectrum (D) measured after 200 K heating shows an asymmetric shape, originating from a small re-appearance of the component at 335.3 eV. Spectrum (E) was taken after heating to 300 K, and its shape was similar to spectra (A) and (B). The intensity changes of each component in these Pd $3d_{5/2}$ spectra described above are summarized in Fig. 1(b). The disappearance of the peak at 335.3 eV correlates to the increase in the component at 335.6 eV. Therefore, we conclude that H_2 exposure caused the chemical shift of the Pd $3d_{5/2}$ core level from 335.3 eV to 335.6 eV. The shift of 0.3 eV is close to the chemical shift induced by adsorbed hydrogen atoms (0.35 eV for the Pd-Cu random alloy surface,[66] and 0.4 eV for the Pd-Cu(111) surface[47]). The re-appearance of the component at 335.3 eV upon heating to 300 K should correspond to the desorption of hydrogen because the adsorbed hydrogen atoms were completely desorbed from the Pd-Cu(111) surface below 300 K.[45,47,67,68] While the component at 335.3 eV was affected by hydrogen, the peak at 335.6 eV observed in spectra (A) and (B) seems not to be changed by hydrogen, judging from the single component in spectrum (C). This result indicates a negligible interaction between the adsorbed hydrogen atoms and the Pd atom at 335.6 eV. The tentative assignment of this component is the Pd atoms located at the subsurface and/or bulk site, which can explain the present experimental results; these Pd atoms do not significantly interact with the adsorbed hydrogen atoms on the Pd-Cu(111) surface.

The single component of spectrum (C) in Fig. 1(a) suggests that the binding energies of the hydrogen-adsorbed Pd and the subsurface Pd are very close. To understand this, we performed a DFT calculation for core level excitation to evaluate the binding energy of the Pd atom at the subsurface site. In our previous DFT study, the binding energy of Pd $3d_{5/2}$ was calculated to be 335.7 and 336.1 eV on a clean and hydrogen-adsorbed Pd-Cu(111) surface, respectively.[47] Here, we performed DFT calculation of the Pd $3d_{5/2}$ core level for a Pd atom placed at the second layer of the Cu(111) slab (a subsurface site). The calculated binding energy was 336.0 eV, which is very close to that of the hydrogen-adsorbed Pd-Cu(111) surface.

Based on the above experimental and theoretical results, we have assigned the component at 335.3 eV and 335.6 eV in Fig. 1(a) to Pd atoms on the surface and the subsurface site, respectively. The model structures of the present Pd-Cu(111) surface are shown in Fig. 1(c). Here, we assumed the coverage of the surface-Pd atoms to be ~0.1 ML, which was equivalent to the prepared Pd-Cu(111) surface.

B: HR-XPS study for the chemical process of HCOOH on Pd-Cu(111)

Next, we investigated the surface chemistry of formic acid because of its significance in CO_2 hydrogenation on Cu surfaces, where formic acid and formate species have been proposed as an important intermediate species in methanol synthesis reaction on Cu-based catalysts.[3,30] Previously, we have systematically investigated the adsorption, desorption, and decomposition processes of formic acid on Cu(111), Cu(997), Cu(977), Zn-Cu(111), and Zn-Cu(997) surfaces using various surface science methods.[15,19,20,22]

Figures 2(a) and (b) show a series of C 1s and O 1s XPS spectra measured on a Pd-Cu(111) surface ($\vartheta_{Pd,\ surface}$ = ~0.05 ML) after formic acid adsorption at 80 K and subsequent heating processes. The coverages of adsorbed species based on the peak area were plotted as a function of heating temperature in Fig. 2(c).

In Fig. 2(a), a single peak for the adsorbed HCOOH molecules was observed at 289.5 eV after HCOOH exposure.[13,19,22] The coverage was estimated to be 0.52 ML, which is higher than the saturation coverage of HCOOH in the first layer on Cu(111) (0.35 ML).[15] Therefore, a multilayer was partly formed on the present surface. After heating to 150 K, the peak area is decreased due to the desorption of the multilayer.[14,15,19,22] In addition, a peak at 288.5 eV is newly observed, attributed to monodentate formate species.[19,22] Heating to 160 K resulted in a further decrease in the HCOOH component and an increase in the monodentate formate component. The coverage of monodentate species after 160 K heating was 0.15 ML. After heating at 300 K, the component at 289.5 eV disappeared and a peak for bidentate formate species was observed at 287.5 eV.[13,19,22] Here, the coverage of bidentate species was estimated to be 0.06 ML, corresponding to 12 % of the initially adsorbed HCOOH. After heating at 450 K, the peak completely disappeared, indicating that bidentate formate species were decomposed and desorbed as H_2 and CO_2.[49,69]

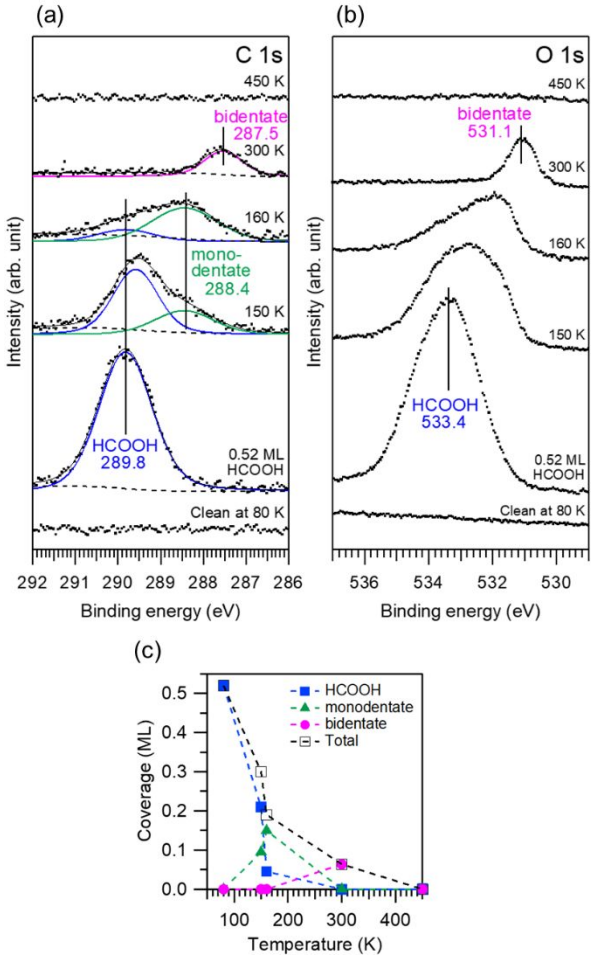

Fig. 2 A series of (a) C 1s and (b) O 1s XPS spectra of HCOOH (0.52 ML) on Pd-Cu(111) at 80 K and after subsequent heating to the indicated temperatures. All spectra were measured at 80 K using a photon energy of 680 eV. The C 1s spectra are fitted by Voigt functions and a Shirley background. (c) Coverages of adsorbed species on Pd-Cu(111) estimated from C 1s peak areas as a function of temperature. The blue, green, and magenta colors indicate molecular HCOOH, monodentate formate, and bidentate formate, respectively.

On the bare Cu(111) surface, monodentate formate species appeared above 160 K, and the coverage at 160 K was less than 0.04 ML.[19] Therefore, the above results indicate that single atom Pd sites catalyse the dissociation of HCOOH to monodentate formate species. However, the conversion ratio of the adsorbed HCOOH to bidentate formate species on Pd-Cu(111) was almost equivalent to that on the Cu(111) surface (13 %).[19] On the present Pd-Cu(111) surface, the coverage of formate species decreased from 0.15 ML to 0.06 ML between 160 K and 300 K. Therefore, some formate species should be decomposed and/or recombinatively desorbed below 300 K. Thus, the Pd atoms embedded in a Cu(111) surface could act as an active site not only for the dissociation of HCOOH but also for the decomposition/recombination of formate.

In the O 1s region, no significant peak was observed on the clean Pd-Cu(111) surface, although the region of the Pd $3p_{3/2}$ core level overlaps with the O 1s region.[70] The absence of a Pd $3p_{3/2}$ peak supports the conjecture that a very small amount of Pd atoms is deposited (0.05 ML), which will be discussed later.

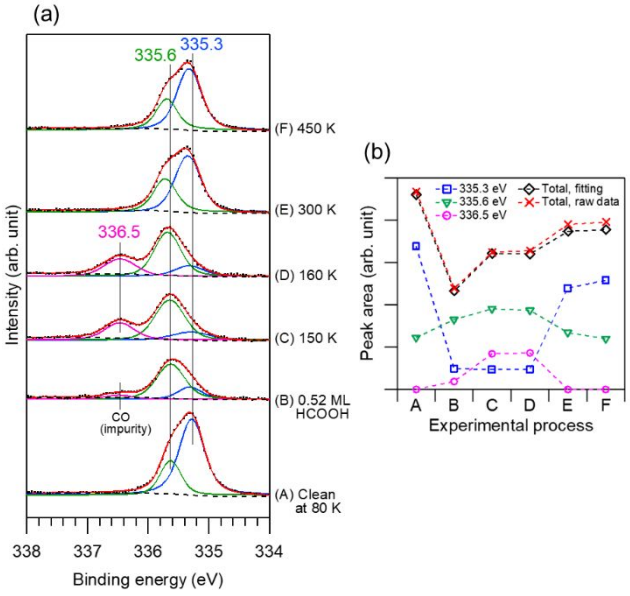

Fig. 3 A series of Pd $3d_{5/2}$ XPS spectra of HCOOH (0.52 ML) on Pd-Cu(111) at 80 K and after subsequent heating to the indicated temperatures. All spectra were measured using a photon energy of 490 eV at 80 K. The spectra are fitted by a Voigt function and a Shirley background. (b) Peak areas of the deconvoluted curves are plotted as a function of the experimental processes indicated in (a).

Upon the adsorption of HCOOH and subsequent heating process, the behaviour of the O 1s spectra was highly consistent with that of C 1s: a single peak for molecular HCOOH at 533.4 eV,[13,19,22] a decrease in the peak of molecular HCOOH and the development of a peak at lower binding energy (monodentate formate) after 150-160 K heating, a single peak for bidentate formate species at 531.1 eV after 300 K heating, [13,19,22] and disappearance of the peak after heating to 450 K. It should be noted that no atomic oxygen signal was observed in O 1s XPS spectra during the present experimental process, indicating that formate (HCOO) species was predominantly decomposed to CO_2 + ½ H_2, which were immediately desorbed. In a previous study, atomic oxygen was observed during the decomposition of formic acid on Pd(111) using high-resolution electron energy loss spectroscopy,[71] interpreted as the involved dehydration process (HCOOH → CO + H_2O). The O 1s spectra in Fig. 2(b) indicate that HCOOH adsorbed on the present Pd-Cu(111) surface was decomposed into only hydrogen and CO_2 (dehydrogenation), the same as that on the Cu(111) surface. In other words, the decomposition process of bidentate formate species on the present Pd-Cu(111) surface was very similar to that on the bare Cu(111) surface. Similar results have been reported on a Pt-Cu(111) single atom alloy surface.[49]

Figure 3(a) shows a series of Pd $3d_{5/2}$ XPS spectra corresponding to the C 1s and O 1s spectra in Fig. 2. In these spectra, three components were observed at 335.3, 335.6, and 336.5 eV. The behaviour of each component was plotted as a function of the experimental process in Fig. 3(b). Spectrum (A) in Fig. 3(a) measured on a clean Pd-Cu(111) surface at 80 K was composed of two components at 335.3 eV and 335.6 eV. These were assigned to the Pd atoms placed on the surface and subsurface, respectively, as discussed in section III-A. Based on

the peak area of the surface component, we estimated the coverage of the surface Pd atoms to be ~0.05 ML in this experiment, ensuring that SAAC was formed on the present Pd-Cu(111) surface.[72–74] Upon the adsorption of HCOOH, the intensity of the surface component significantly decreased (spectrum (B)), indicating that the surface Pd atoms interacted with HCOOH. The additional component at 336.5 eV is probably due to impurity. The most plausible candidate is CO based on the 1.3 eV chemical shift reported for the CO-adsorbed Pd(111)[75] surface and our DFT calculations (shown in Table 3). We did not detect the signal of CO in the C 1s and O 1s regions due to its very low coverage (estimated to be ~0.003 ML based on the Pd $3d_{5/2}$ component). Heating to 150 and 160 K resulted in an increase in the components at 335.6 and 336.5 eV and a decrease in the 335.3 eV component. The C 1s spectra in Fig. 2 show that monodentate formate species were formed after 150-160 K heating. Therefore, the increase in these components should be related to the formation of monodentate formate species and dissociated hydrogen atoms (HCOOH → $HCOO_{ad}$ + H_{ad}), which will be discussed in the following section. Note that the total intensity recovered due to the desorption of molecular HCOOH species. After heating to 300 K, the component at 336.5 eV disappeared probably due to the recombinative desorption of hydrogen and the transformation of monodentate formate to bidentate formate species (see Fig. 1 and Fig. 2), as well as the desorption of CO.[67] These processes could lead to an increase in the total intensity. In addition, the peak at 335.6 eV decreased to a similar intensity in spectrum (A). The intensity of the surface Pd component (335.3 eV) increased but was lower than that in spectrum (A), indicating that some surface Pd atoms might be occupied by bidentate formate species. Spectrum (F) was measured on the surface after heating to 450 K, which corresponds to the clean surface because bidentate formate species were completely decomposed at 450 K (see Fig. 2). However, the shapes of spectra (F) and (A) were different, i.e., the peak area of the surface Pd atoms decreased while that of the component at 335.6 eV was almost equal. The decrease in the surface component indicates that some of the surface Pd atoms could migrate to the subsurface or bulk site upon heating to higher temperature above ~400 K.[46,48,65] Although such migration could cause an increase in the subsurface component, the almost equal intensity for the peak at 335.6 eV may be rationalized by migration to the deeper layers than the present probing depth (~5.5 Å with a photon energy of 490 eV).

C: DFT calculations for the chemical process of HCOOH and formate species on Pd-Cu(111)

The observed core level shifts of Pd $3d_{5/2}$ in Fig. 3 indicate that the Pd single atom sites play a specific role in the chemical process of HCOOH on the present Pd-Cu(111) surface. To investigate the interaction between the Pd sites and adsorbed species, we have conducted DFT calculations including geometry optimization and core-level excitation for Pd $3d_{5/2}$. First, we explore the stable adsorption structure of HCOOH and formate species on a Pd-Cu(111) surface. Figures 4 and 5 show various model structures for the HCOOH and formate species on the Pd-Cu(111) surface, respectively. Note that the calculations of HCOOH are conducted for only a trans-form molecule because it is more stable than a cis-form molecule.[31] The configurations in Figs. 4(c) and (d) are almost inverse to those in Figs. 4(a) and (b), i.e., the hydroxyl H atom contacts with the Pd atom, and the carbonyl oxygen atom is located at a Cu-Cu bridge site (Fig. 4(c)) or an on-top Cu site (Fig. 4(d)). The adsorption energies, ΔH_{ad}, for the structures in Fig. 4 are summarized in Table 1, where the total energy of gaseous HCOOH is defined as 0 eV. For comparison, ΔH_{ad} on Cu(111) with a configuration corresponding to Fig. 4(a) is also shown. Previous theoretical studies have reported that such a configuration is the most stable structure for a single HCOOH molecule adsorbed on Cu(111).[31,33,35,76] The present calculation resulted in ΔH_{ad} of −0.46 eV for HCOOH on a bare Cu(111) surface, which was within the range of previously reported values including van der Waals interaction.[33,35] ΔH_{ad} on Pd-Cu(111) shows that an HCOOH molecule is more strongly adsorbed at a Pd single atom site than a bare Cu site, except for the configuration in Fig. 4(c). Although the structure in Fig. 4(d) is the most stable, its adsorption energy is very close to those for the other configurations in Figs. 4(a) and (b). It is noteworthy that the polymerization of HCOOH via a hydrogen-bonding network stabilizes the adsorbed HCOOH layer,[15,34] but such an effect was not considered in the present calculations.

Figure 5 shows the structure models of monodentate and bidentate formate species adsorbed on the Pd-Cu(111) surface. The calculated adsorption energies with respect to gaseous CO_2 and ½ H_2 molecules (decomposed products of formate species) are summarized in Table 2 together with the results on the bare Cu(111) surface. The adsorption sites for the formate species on the bare Cu(111) surface are described in brackets next to ΔH_{ad}

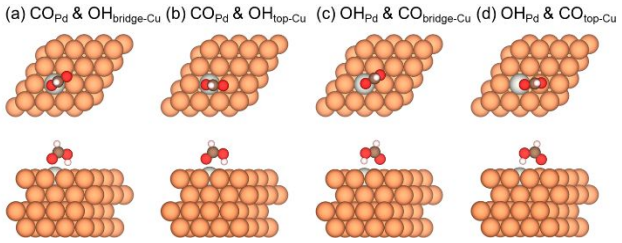

Fig. 4 Optimized structures of HCOOH adsorbed on Pd-Cu(111). The configuration of the molecule is represented by functional groups with subscripts standing for their bonding site. The orange, grey, black, red, and white spheres represent Cu, Pd, C, O, and H atoms, respectively.

Table 1 Calculated adsorption energies of adsorbed HCOOH on Pd-Cu(111) with the configurations shown in Fig. 4. The adsorption energy on Cu(111) was calculated with the configuration corresponding to Fig. 4(a). The indicated values are with respect to a gaseous *trans*-HCOOH molecule.

Configuration	ΔH_{ad} (eV)	
	Pd-Cu(111)	Cu(111)
CO_{Pd} & $OH_{bridge\text{-}Cu}$ (Fig. 4(a))	−0.54	−0.46
CO_{Pd} & $OH_{top\text{-}Cu}$ (Fig. 4(b))	−0.53	
OH_{Pd} & $CO_{bridge\text{-}Cu}$ (Fig. 4(c))	−0.44	
OH_{Pd} & $CO_{top\text{-}Cu}$ (Fig 4(d))	−0.55	

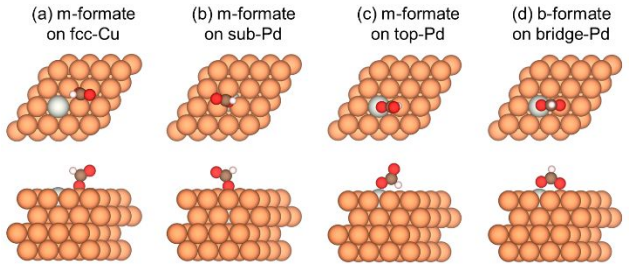

Fig. 5 Optimized structures of (a)-(c) monodentate and (d) bidentate formate species adsorbed on Pd-Cu(111); the upper and lower models are the top view and side view, respectively. The orange, gray, black, red, and white spheres represent Cu, Pd, C, O, and H atoms, respectively.

Table 2 Calculated adsorption energies (ΔH_{ad}) of monodentate and bidentate formate species adsorbed on Pd-Cu(111) with the configurations shown in Fig. 5. The calculations on Cu(111) were performed with the configuration described in the brackets. The indicated values are with respect to CO_2 (g) + ½ H_2 (g), which are the desorbed gaseous products from an adsorbed formate species at high temperature.

Configuration	ΔH_{ad} (eV)	
	Pd-Cu(111)	Cu(111)
m-formate on fcc-Cu (Fig. 5(a))	−0.53	−0.55 (m-formate on fcc-Cu)
m-formate on sub-Pd (Fig. 5(b))	−0.35	
m-formate on top-Pd (Fig. 5(c))	+0.02	
b-formate on bridge-Pd (Fig. 5(d))	−0.82	−0.91 (b-formate on bridge-Cu)

values in the table. In Fig. 5 and Table 2, monodentate and bidentate formate species are denoted as m-formate and b-formate, respectively. The present ΔH_{ad} values on Cu(111) were close to those in two previous studies.[33,35]

For monodentate formate species, the most stable adsorption site is an fcc hollow site consisting of three Cu atoms, where the adsorption energy was close to that on the bare Cu(111) surface. Because monodentate formate species favour a three-fold hollow site rather than bridge and on-top sites,[33,35] we locate monodentate species at an hcp hollow site above a subsurface Pd atom (Fig. 5(b)). ΔH_{ad} for the structure in Fig. 5(b) was −0.35 eV, less stable than that for the structure in Fig. 5(a) (−0.53 eV). When monodentate formate was located on a hollow site involving a Pd atom and two Cu atoms, the molecule spontaneously transformed into a bidentate configuration during geometry optimization (not shown here). The structure in Fig. 5(c), where monodentate formate occupies an on-top site of Pd, was unstable (+0.02 eV). In the case of bidentate formate species, the configuration bridged between Pd and Cu atoms (Fig. 5(d)) was less stable than the bridged structure on the bare Cu(111) surface. It is noted that ΔH_{ad} for bidentate formate at the Cu-Cu bridge site around a Pd atom was calculated to be −0.90 eV (not shown here), which was almost equivalent to that on a bare Cu surface. Furthermore, if bidentate formate was initially placed on the on-top Pd (i.e., two oxygen atoms in formate are bonding to a Pd atom), geometry optimization resulted in the migration of formate to a bridged configuration. These results clearly indicate that bidentate formate species are preferentially adsorbed on Cu bridge sites rather than on Pd-inclusive sites. This tendency is consistent with the previous experimental results; the decomposition temperature of bidentate formate species on CuPd(110) is lower than those on pure Cu surfaces.[69]

We also calculated ΔH_{ad} for the co-adsorbed configuration of one monodentate formate species and a dissociated hydrogen atom. In Fig. 6, monodentate formate species occupy the fcc hollow site, i.e., the same as Fig. 5(a), and H atoms are placed on the fcc hollow sites consisting of two Cu atoms and one Pd atom. Figures 6(a) and (b) show the optimized structures of one monodentate formate and one hydrogen atom on a Pd-Cu(111) surface. The configuration in Fig. 6(a), where the H atom and monodentate formate were far away from each other, was more favourable than that in Fig. 6(b) (−0.26 eV for Fig. 6(a) and −0.17 eV for Fig. 6(b) with respect to a gaseous trans-HCOOH molecule). These calculated results show that the co-adsorption of a monodentate formate species and a hydrogen atom is less stable than molecularly adsorbed HCOOH (see Table 1), indicating that an isolated monodentate formate is metastable. Note that previous experimental and theoretical studies have reported that monodentate species are stabilized by linking with adsorbed molecules via hydrogen bonding on Cu(111).[13,15,20,35,77]

Here, we assumed the dimer- and trimer-like configurations shown in Figs. 6(c) and (d) to investigate the origin of the Pd $3d_{5/2}$ core level shift observed in the HR-XPS measurements (Fig. 3), which will be discussed in the following section. In the structures of Figs. 6(c) and (d), all atoms were fixed in their initial positions because formate species transformed into the bidentate form during geometry optimization in these configurations; we excluded the co-adsorbed configuration of bidentate formate and H, because in reality the dissociated H atoms were desorbed from the Pd-Cu(111) surface below the temperature at which bidentate species can be formed.[45,47,67,68]

We performed DFT calculations for Pd $3d_{5/2}$ core level excitation to interpret the observed XPS spectra based on the present theoretical models. Table 3 shows the calculated binding energies (CBEs) for a clean Pd-Cu(111) surface and the adsorption structures in Figs. 4-6. The CBEs are estimated by the ΔSCF method.[63] The value for a clean Pd-Cu(111) surface was referenced from our previous study.[47] The CBE for the CO-adsorbed Pd-Cu(111), which was observed as impurity in Fig. 3, was also shown in Table 3.

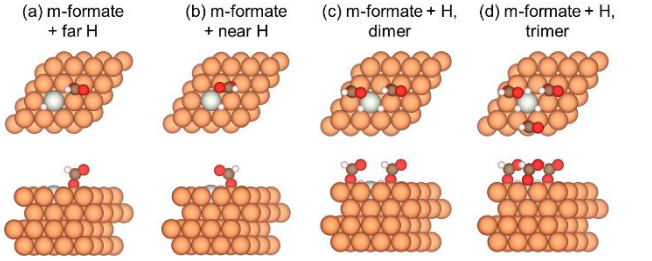

Fig. 6 Structure models for the co-adsorption of monodentate formate species and dissociated hydrogen atoms. (a) and (b) are geometrically optimized, and their adsorption energies are −0.26 eV and −0.17 eV with respect to the gaseous HCOOH molecule, respectively. In (c) and (d), all atoms are fixed in their initial positions. The upper and lower models represent the top view and side view, respectively.

Table 3 Calculated binding energies (CBEs) of Pd $3d_{5/2}$ for the adsorption structures shown in Figs. 4-6. ΔCBE in the last column is the difference of the CBE from the clean surface.

Adsorbate	Configuration	CBE (eV)	ΔCBE (eV)
clean	surface	335.7	-
	subsurface	336.0	0.3
HCOOH	CO_{Pd} & $OH_{bridge\text{-}Cu}$ (Fig. 4(a))	335.7	0.0
	CO_{Pd} & $OH_{top\text{-}Cu}$ (Fig. 4(b))	335.7	0.0
	OH_{Pd} & $CO_{bridge\text{-}Cu}$ (Fig. 4(c))	335.8	0.1
	OH_{Pd} & $CO_{top\text{-}Cu}$ (Fig. 4(d))	335.8	0.1
formate	m-formate, fcc-Cu (Fig. 5(a))	335.7	0.0
	m-formate, sub-Pd (Fig. 5(b))	336.0	0.3
	b-formate, bridge-Pd (Fig. 5(c))	335.7	0.0
formate + H	far (Fig. 6(a))	335.9	0.2
	near (Fig. 6(b))	335.8	0.1
	dimer (Fig. 6(c))	336.2	0.5
	trimer (Fig. 6(d))	336.5	0.8
CO	on-top of Pd	336.5	0.8

In the case of HCOOH adsorption, the chemical shift of the Pd $3d_{5/2}$ core level (ΔCBE) depends on functional group bonding to the Pd atom; adsorption via carbonyl oxygen (Figs. 4(a) and (b)) little alters the binding energy of Pd $3d_{5/2}$, while the hydroxyl hydrogen atom causes a small chemical shift (0.1 eV for Figs. 4(c) and (d)). These results indicate that HCOOH could chemically interact with the Pd atom embedded in the Cu(111) surface via its hydroxyl hydrogen. In the Pd $3d_{5/2}$ spectra, the surface component significantly decreased upon HCOOH adsorption (see Fig. 3), indicating that some of the surface Pd atoms chemically interact with the adsorbed HCOOH molecule, i.e., they are covered with the adsorbed species. This molecule may be adsorbed with the configuration in Fig. 4(d) because it is more stable than that in Fig. 4(c). Unfortunately, for spectra (B)-(D) in Fig. 3(a), deconvolution including the HCOOH-adsorbed component is difficult due to the small chemical shift and broadness of these spectra.

In the case of possible monodentate formate structures, ΔCBEs are negligibly small. This is not surprising because monodentate formate is not directly bonded to the Pd atom in Figs. 5(a) and (b). Bidentate formate species also induce a negligible shift of the CBE in Pd $3d_{5/2}$, despite the bridged structure between Pd and Cu (Fig. 5(d)). This suggests that the observed Pd $3d_{5/2}$ spectra do not support the assumption of a stable adsorption site of bidentate formate species at the Pd-inclusive site on a dilute alloy Pd-Cu(111) surface. Thus, we conclude that bidentate formate species prefer the Cu-Cu bridge site even on a Pd-Cu(111) surface because of the more stable adsorption energy at a Cu-Cu bridge site compared with a Pd-Cu bridge site (see Table 2). A previous experimental study has also reported the lower stability of bidentate formate species on a CuPd(110) surface than on Cu(110).[69] Note that a recent theoretical study reported that a Pd-Cu bridge site is a stable adsorption site at 298 K based on their calculated Gibbs free energies.[78] This implies that the favourable adsorption site of bidentate formate species at reaction conditions (~500 K is a typical temperature for methanol synthesis) is different from that under the present experimental conditions at lower temperature; the entropic effect may become significant at higher temperature.

On the co-adsorbed surfaces of monodentate formate and the dissociated H atom, which corresponds to the surface after heating to 150-160 K in section III-B, the CBE of Pd $3d_{5/2}$ significantly shifts to a higher value. For the configuration in Fig. 6(a), the ΔCBE is 0.2 eV. This shift is almost equivalent to that for the surface with one adsorbed hydrogen atom.[47] Therefore, in the configuration in Fig. 6(a), the chemical shift of Pd $3d_{5/2}$ is essentially induced by the hydrogen atom. This is associated with a negligible shift on only the monodentate formate-adsorbed surface (Fig. 5(a)). For the dimer and trimer structures (Figs. 6(c) and (d)), the ΔCBEs are 0.5 and 0.8 eV, respectively. We have previously reported that the chemical shift induced by two and three hydrogen atoms on the isolated Pd atom was 0.4 eV and 0.5 eV, respectively. [47] The present calculations included not only hydrogen but also monodentate formate species, and the results show significantly higher chemical shifts than in the case of only hydrogen atoms. Interestingly, if the adsorbed H atoms are removed from the structure in Fig. 6(c), the ΔCBE becomes negligibly small. Therefore, we conclude that the synergy effect by the H atoms and monodentate formate species around the isolated Pd site induces significant shifts of Pd $3d_{5/2}$. In section III-B, we explained that the component at 336.5 eV in the Pd $3d_{5/2}$ XPS spectra relates to monodentate formate species and dissociated H atoms. The peak areas of the XPS spectra in Fig. 2 and Fig. 3 show that the coverage of monodentate formate species was at least three times larger than that of Pd, suggesting that structures such as in Figs. 6(c) and (d) can be locally formed. Therefore, we conclude that the Pd $3d_{5/2}$ peak at 336.5 eV originates from the aggregate structure of monodentate formate species and the dissociated H atoms around the Pd atom. The previous STM observations reported that a cluster formation of formate species was observed on Cu(111).[14,20]

To clarify the origin of the Pd $3d_{5/2}$ core-level shift, we performed Mulliken charge population analysis on the substrate and adsorbed species, and the results are summarized in Table 4. Here, we chose O atom bonding to the surface as a representation of monodentate formate species. The values in brackets are the results of the same analysis on a bare Cu(111) surface. On a clean Pd-Cu(111) surface, the charge on the Pd atom decreases from its neutral state, while that of surface Cu atoms increases. This is ascribed to the charge transfer from Pd to Cu, as we have previously reported.[47] On a hydrogen- and formate-co-adsorbed surface, the valence electrons of the Pd and Cu atoms are less than those of a clean Pd-Cu(111) surface. This indicates the charge transfer from the substrate to the adsorbates. The increase in the number of H atoms and formate species resulted in a systematic decrease of the charge on Pd, particularly 4d electrons (0.08 decrease in total, and 0.19

Table 4 Mulliken charge populations in Pd, Cu, H, and O atoms. For Cu, the values are the average of the atoms surrounding the Pd atom. The column of H_{dis} shows the average value of the charge on the dissociated H atoms. O_{bond} represents the oxygen atom directly bonding to the metal surface in formate species.

Configuration		Pd		Cu_{surf}	H_{dis}	O_{bond}
		Total	4d			
neutral		16	9	19	1	6
clean		15.86	9.24	19.11 (19.10)	-	-
m-formate	far H	15.84	9.20	19.09 (19.07)	1.19 (1.15)	6.41 (6.41)
	dimer	15.79	9.13	19.07 (19.05)	1.15 (1.14)	6.41 (6.41)
	trimer	15.78	9.05	19.05 (19.02)	1.13 (1.11)	6.40 (6.40)

decrease in the 4d electrons). This charge depression should be related to the significant chemical shift of Pd $3d_{5/2}$. In the case of Cu, the averaged charge decreases from 19.11 to 19.05. Thus, Pd donates more electrons to the adsorbates (formate and hydrogen) than Cu atoms.

On a bare Cu(111) surface, H atoms have fewer electrons than those on a Pd-Cu(111) surface (1.11 for Cu(111) and 1.13 for Pd-Cu(111), respectively). The charge on O atoms is almost independent of the presence of Pd. These results indicate that the electron transfer from a bare Cu(111) surface to the adsorbates is lower than that from a Pd-Cu(111) surface (or at least almost equivalent). However, on a bare Cu(111) surface, the valence electrons on the Cu atoms are fewer than those on a Pd-Cu(111) surface. This means that the Cu atoms on a bare Cu(111) surface, despite the lower electron transfer , lose more electrons upon hydrogen and formate adsorption than those on a Pd-Cu(111) surface. This discrepancy can be rationalized by considering the charge on the Pd atom. On a surface with a trimer-like structure of hydrogen and monodentate formate species (Fig. 6(d)), the total charge on the Pd atom decreases to 15.78, which is slightly less than that on a three-hydrogen-adsorbed Pd-Cu(111) surface (15.80).[47] The lower charge of the Pd atom on the co-adsorbed surface of hydrogen and formate indicates the charge transfer from Pd to monodentate formate species. Since formate species are far away from the Pd atom, such electron transfer occurs through the Cu substrate. This interpretation is associated with the results that the Cu atoms on a Pd-Cu(111) surface have more valence electrons than those on a bare Cu(111) surface. We conclude that this indirect charge transfer from the Pd atom to monodentate formate species via the Cu substrate is the origin of the significant chemical shift of Pd $3d_{5/2}$ observed in Fig. 3(a).

Based on the present experimental and theoretical results, the chemical process of formic acid on the present Pd-Cu(111) surface is summarized as follows. After the incident collision and transient migration of a formic acid molecule on the surface at 80 K, the molecule would be preferentially adsorbed on the single atom Pd site via its hydroxyl hydrogen atom. When the HCOOH-adsorbed surface was heated to 150 K, HCOOH molecules including the multilayer were desorbed, and some of the rest of the molecules were dissociated into monodentate formate species (0.15 ML) and hydrogen atoms. Monodentate formate species and dissociated H atoms would aggregate around the Pd site to form a cluster-like structure, as shown in Figs. 6(c) and (d). Heating to 160 K further proceeded the HCOOH desorption and formation of the cluster. After 300 K heating, the H atoms were completely desorbed as H_2, and bidentate formate species (0.06 ML) were formed and preferentially occupied the bridging site consisting of two Cu atoms. Therefore, the Pd site should be unoccupied at 300 K. Heating to 450 K resulted in the complete decomposition of formate species into CO_2 + H (=½ H_2), which were immediately desorbed. The migration of some Pd atoms from the surface into the subsurface/bulk site also occurred above ~430 K.[46,48]

The present study found that the surface chemistry of bidentate formate species on a dilute alloy Pd-Cu(111) surface is almost identical that on a bare Cu(111) surface because of the weak interaction between formate species and the Pd atom. On the present Pd-Cu(111) surface, bidentate formate species are preferably adsorbed on the Cu sites and do not affect the reactivity of the Pd site. This suggests that single atom alloy Pd-Cu(111) would have excellent activity for H_2 dissociation even when formate species exist on the Pd-Cu(111) surface.[2,3] A single atom alloy catalyst may overcome the low activity for H_2 dissociation of the current Cu-based catalyst,[5] which leads to lowering the operation temperature of methanol synthesis.

IV. Summary

We systematically investigated the interaction of H_2 and HCOOH with a dilute alloy Pd-Cu(111) surface using HR-XPS and DFT calculations. Important results and conclusions are summarized as follows.

(1) The Pd $3d_{5/2}$ spectrum on the clean surface consisted of two components, 335.3 eV and 335.6 eV, which are attributed to surface Pd and subsurface Pd, respectively. The prepared Pd-Cu(111) surface had low coverage of surface Pd atoms (0.05 ML) and acted as a single atom alloy catalyst.

(2) On the HCOOH-adsorbed Pd-Cu(111) surface, the Pd $3d_{5/2}$ spectrum showed a significant chemical shift upon heating to 160 K. This shift correlated well to the C 1s peak assigned to monodentate formate species. After heating up to 300 K, only bidentate formate species remained on the surface. The amount of bidentate species was 12 % of the initial HCOOH coverage, almost equivalent to the case on Cu(111). Heating to 450 K resulted in the decomposition of bidentate formate and desorption as CO_2 + ½ H_2.

(3) Systematic DFT calculations were performed to explore the stable adsorption structures of HCOOH and formate species. The calculated results show that HCOOH prefers the Pd site, while formate species are favourably adsorbed on the Cu site. This means that the Pd site is unoccupied on a formate-adsorbed Pd-Cu(111) surface. The DFT results for core-level excitation show that both monodentate and bidentate formate species little affect the binding energy of Pd $3d_{5/2}$. On the other hand, the aggregation of monodentate formate and dissociated

hydrogen atoms around the Pd site caused a significant chemical shift in Pd $3d_{5/2}$. Thus, the observed shift of Pd $3d_{5/2}$ originates from the aggregate structure of monodentate formate and hydrogen atoms.

(4) The present Pd-Cu(111) surface has an advantage during CO_2 hydrogenation; the Pd site can act as the H_2 dissociation site without poisoning by formate intermediate species. In addition, we expect that a Pd-Cu single atom alloy catalyst may lower the reaction temperature compared with the typical methanol synthesis condition using a Cu/ZnO catalyst, which requires an operation temperature of 500 K because of its low activity of hydrogen activation. This proposal will be demonstrated in our forthcoming paper, in which the CO_2 hydrogenation process on a single atom alloy Pd-Cu(111) surface has been observed at relatively low temperature using ambient-pressure XPS.

Author Contributions

W. O.: theoretical investigation, visualization, writing - original draft, and writing – review & editing; M. H.: experimental investigation; Y. S.: experimental investigation; K. M.: experimental investigation; S. Y.: experimental investigation; S. T.: investigation; M. K.: software and theoretical investigation; T. O.: calculational resources, software, and theoretical investigation; J. Y.: funding acquisition, supervision, investigation, writing – original draft, and writing – review & editing.

Conflicts of interest

There are no conflicts to declare.

Data availability

Data for this article, including raw XPS spectra and outputs of DFT calculations are available at ScienceDB at https://doi.org/10.57760/sciencedb.14315.

Acknowledgements

The present study was supported by the Advanced Catalytic Transformation program for Carbon utilization (ACT-C) of the Japan Science and Technology Agency (JST), a Grant-in-Aid for Scientific Research on Innovative Areas “3D Active-Site Science” (17H05212) and “Hydrogenomics” (1805517), and JST CREST (JPMJCR20R4). The HR-XPS experiments were performed at Photon Factory BL-13B under PF-PAC approval (No. 2015-S2-008). We are grateful to Prof. Kazuhiko Mase and the staff members of Photon Factory for their technical support.

References

1 X. Nie, W. Li, X. Jiang, X. Guo and C. Song, in *Advances in Catalysis*, ed. C. Song, Elsevier Inc., 2019, vol. 65, pp. 121–233.

2 X. Jiang, X. Nie, X. Guo, C. Song and J. G. Chen, Recent Advances in Carbon Dioxide Hydrogenation to Methanol via Heterogeneous Catalysis, *Chem. Rev.*, 2020, **120**, 7984–8034.

3 J. Zhong, X. Yang, Z. Wu, B. Liang, Y. Huang and T. Zhang, State of the art and perspectives in heterogeneous catalysis of CO_2 hydrogenation to methanol, *Chem. Soc. Rev.*, 2020, **49**, 1385–1413.

4 K. Stangeland, H. Li and Z. Yu, CO_2 hydrogenation to methanol: the structure–activity relationships of different catalyst systems, *Energy, Ecol. Environ.*, 2020, **5**, 272–285.

5 M. M. Li and S. C. E. Tsang, Bimetallic catalysts for green methanol production via CO_2 and renewable hydorgen: a mini-review and prospects, *Ctalysis Sci. Thechnology*, 2018, **8**, 3450–3464.

6 T. Koitaya, S. Yamamoto, I. Matsuda and J. Yoshinobu, Surface chemistry of carbon dioxide on copper model catalysts studied by ambient-pressure X-ray photoelectron spectroscopy, *e-Journal Surf. Sci. Nanotechnol.*, 2019, **17**, 169–178.

7 J. Niu, H. Liu, Y. Jin, B. Fan and W. Qi, ScienceDirect Comprehensive review of Cu-based CO 2 hydrogenation to CH 3 OH : Insights from experimental work and theoretical analysis, *Int. J. Hydrogen Energy*, 2022, **47**, 9183–9200.

8 P. S. Murthy, W. Liang, Y. Jiang and J. Huang, Cu-Based Nanocatalysts for CO_2Hydrogenation to Methanol, *Energy and Fuels*, 2021, **35**, 8558–8584.

9 R. J. Madix, The adsorption and reaction of simple molecules on metal surfaces, *Surf. Sci.*, 1979, **89**, 540–553.

10 B. A. Sexton, Observation of formate species on a copper (100) surface by high resolution electron energy loss spectroscopy, *Surf. Sci.*, 1979, **88**, 319–330.

11 I. Nakamura, H. Nakano, T. Fujitani, T. Uchijima and J. Nakamura, Synthesis and decomposition of formate on Cu(111) and Cu(110) surfaces: Structure sensitivity, *J. Vac. Sci. Technol. A*, 1999, **17**, 1592.

12 A. Sotiropoulos, P. K. Milligan, B. C. C. Cowie and M. Kadodwala, Structural study of formate on Cu(111), *Surf. Sci.*, 2000, **444**, 52–60.

13 A. E. Baber, K. Mudiyanselage, S. D. Senanayake, A. Beatriz-Vidal, K. A. Luck, E. C. H. Sykes, P. Liu, J. A. Rodriguez and D. J. Stacchiola, Assisted deprotonation of formic acid on Cu(111) and self-assembly of 1D chains, *Phys. Chem. Chem. Phys.*, 2013, **15**, 12291–12298.

14 M. D. Marcinkowski, C. J. Murphy, M. L. Liriano, N. A. Wasio, F. R. Lucci and E. C. H. Sykes, Microscopic View of the Active Sites for Selective Dehydrogenation of Formic Acid on Cu(111), *ACS Catal.*, 2015, **5**, 7371–7378.

15 Y. Shiozawa, T. Koitaya, K. Mukai, S. Yoshimoto and J. Yoshinobu, Quantitative analysis of desorption and decomposition kinetics of formic acid on Cu(111): The importance of hydrogen bonding between adsorbed species, *J. Chem. Phys.*, 2015, **143**, 234707.

16 J. Quan, T. Kondo, G. Wang and J. Nakamura, Energy Transfer Dynamics of Formate Decomposition on Cu(110), *Angew. Chemie - Int. Ed.*, 2017, **56**, 3496–3500.

17 T. Koitaya, S. Yamamoto, Y. Shiozawa, Y. Yoshikura, M. Hasegawa, J. Tang, K. Takeuchi, K. Mukai, S. Yoshimoto, I. Matsuda and J. Yoshinobu, CO_2 Activation and Reaction on Zn-Deposited Cu Surfaces Studied by Ambient-Pressure X-ray Photoelectron Spectroscopy, *ACS Catal.*, 2019, **9**, 4539–4550.

18 J. Quan, F. Muttaqien, T. Kondo, T. Kozarashi, T. Mogi, T. Imabayashi, Y. Hamamoto, K. Inagaki, I. Hamada, Y. Morikawa and J. Nakamura, Vibration-driven reaction of CO_2 on Cu surfaces via Eley–Rideal-type mechanism, *Nat. Chem.*, 2019, **11**, 722–729.

19 Y. Shiozawa, T. Koitaya, K. Mukai, S. Yoshimoto and J. Yoshinobu, The roles of step-site and zinc in surface chemistry of formic acid on clean and Zn-modified Cu(111) and Cu(997) surfaces studied by HR-XPS, TPD, and IRAS, *J. Chem. Phys.*, 2020, **152**, 044703.

20 A. Shiotari, S. E. M. Putra, Y. Shiozawa, Y. Hamamoto, K. Inagaki, Y. Morikawa, Y. Sugimoto, J. Yoshinobu and I. Hamada, Role of Intermolecular Interactions in the Catalytic Reaction of Formic Acid on Cu(111), *Small*, 2021, **17**, 2008010.

21 M. Bowker and R. J. Madix, XPS, UPS and thermal desorption studies of the reactions of formaldehyde and formic acid with the Cu(110) surface, *Surf. Sci.*, 1981, **102**, 542–565.

22 W. Osada, S. Tanaka, K. Mukai, Y. H. Choi and J. Yoshinobu, Adsorption, Desorption, and Decomposition of Formic Acid on Cu (977): The Importance of Facet of the Step, *J. Physcal Chem. C*, 2022, **126**, 8354–8363.

23 B. E. Hayden, K. Prince, D. P. Woodruff and A. M. Bradshaw, An IRAS study of formic acid and surface formate adsorbed on Cu(110), *Surf. Sci.*, 1983, **133**, 589–604.

24 J. Stohr, D. A. Outka, R. J. Madix and U. Dobler, Evidence for a Novel Chemisorption Bond: Formate (HCO_2) on Cu(100), *Phys. Rev. Lett.*, 1985, **54**, 1256–1259.

25 D. A. Outka, R. J. Madix and J. Stöhr, Structural studies of formate and methoxy groups on the Cu(100) surface using NEXAFS and SEXAFS, *Surf. Sci.*, 1985, **164**, 235–259.

26 L. H. Dubois, T. H. Ellis, B. R. Zegarski and S. D. Kevan, New insights into the kinetics of formic acid decomposition on copper surfaces, *Surf. Sci.*, 1986, **172**, 385–397.

27 M. D. Crapper, C. E. Riley, D. P. Woodruff, A. Puschmann and J. Haase, Determination of the adsorption structure for formate on Cu(110) using SEXAFS and NEXAFS, *Surf. Sci.*, 1986, **171**, 1–12.

28 D. P. Woodruff, C. F. McConville, A. L. D. Kilcoyne, T. Lindner, J. Somers, M. Surman, G. Paolucci and A. M. Bradshaw, The structure of the formate species on copper surfaces: new photoelectron diffraction results and sexafs data reassessed, *Surf. Sci.*, 1988, **201**, 228–244.

29 M. Bowker, S. Haq, R. Holroyd, P. M. Parlett, S. Poulston and N. Richardson, Spectroscopic and kinetics studies of formic acid adsorption on Cu(110), *J. Chem. Soc. Faraday Trans.*, 1996, **92**, 4683–4686.

30 M. Behrens, F. Studt, I. Kasatkin, S. Kühl, M. Hävecker, F. Abild-pedersen, S. Zander, F. Girgsdies, P. Kurr, B. Kniep, M. Tovar, R. W. Fischer, J. K. Nørskov and R. Schlögl, The active site of methanol synthesis over $Cu/ZnO/Al_2O_3$ inductrial catalysts, *Science.*, 2012, **336**, 893–898.

31 A. Chutia, I. P. Silverwood, M. R. Farrow, D. O. Scanlon, P. P. Wells, M. Bowker, S. F. Parker and C. R. A. Catlow, Adsorption of formate species on Cu(*h,k,l*) low index surfaces, *Surf. Sci.*, 2016, **653**, 45–54.

32 F. Muttaqien, H. Oshima, Y. Hamamoto, K. Inagaki, I. Hamada and Y. Morikawa, Desorption dynamics of CO_2 from formate decomposition on Cu(111), *Chem. Commun.*, 2017, **53**, 9222–9225.

33 S. E. M. Putra, F. Muttaqien, Y. Hamamoto, K. Inagaki, I. Hamada and Y. Morikawa, Van der Waals density functional study of formic acid adsorption and decomposition on Cu(111), *J. Chem. Phys.*, 2019, **150**, 154707.

34 S. E. M. Putra, F. Muttaqien, Y. Hamamoto, K. Inagaki, A. Shiotari, J. Yoshinobu, Y. Morikawa and I. Hamada, Theoretical study on adsorption and reaction of polymeric formic acid on the Cu(111) surface, *Phys. Rev. Mater.*, 2021, **5**, 075801.

35 B. W. J. Chen, S. Bhandari and M. Mavrikakis, Role of Hydrogen-bonded Bimolecular Formic Acid-Formate Complexes for Formic Acid Decomposition on Copper: A Combined First-Principles and Microkinetic Modeling Study, *ACS Catal.*, 2021, **11**, 4349–4361.

36 A. Karelovic, G. Galdames, J. C. Medina, C. Yévenes, Y. Barra and R. Jiménez, Mechanism and structure sensitivity of methanol synthesis from CO_2 over SiO_2-supported Cu nanoparticles, *J. Catal.*, 2019, **369**, 415–426.

37 J. Eppinger and K. W. Huang, Formic Acid as a Hydrogen Energy Carrier, *ACS Energy Lett.*, 2017, **2**, 188–195.

38 T. Inui and T. Takeguchi, EFFECTIVE CONVERSION OF CARBON DIOXIDE AND HYDROGEN TO HYDROCARBONS, *Catal. Today*, 1991, **10**, 95–106.

39 T. Inui, H. Hara, T. Takeguchi and J. B. Kim, Structure and function of Cu-based composite catalysts for highly effective synthesis of methanol by hydrogenation of CO_2 and CO, *Catal. Today*, 1997, **36**, 25–32.

40 X. Jiang, N. Koizumi, X. Guo and C. Song, Bimetallic Pd-Cu catalysts for selective CO_2 hydrogenation to methanol, *Appl. Catal. B Environ.*, 2015, **170–171**, 173–185.

41 X. Nie, X. Jiang, H. Wang, W. Luo, M. J. Janik, Y. Chen, X. Guo and C. Song, Mechanistic Understanding of Alloy Effect and Water Promotion for Pd-Cu Bimetallic Catalysts in CO_2 Hydrogenation to Methanol, *ACS Catal.*, 2018, **8**, 4873–4892.

42 X. Jiang, X. Nie, X. Wang, H. Wang, N. Koizumi, Y. Chen, X. Guo and C. Song, Origin of Pd-Cu bimetallic effect for synergetic promotion of methanol formation from CO_2 hydrogenation, *J. Catal.*, 2019, **369**, 21–32.

43 R. T. Hannagan, G. Giannakakis, M. Flytzani-Stephanopoulos and E. C. H. Sykes, Single-Atom Alloy Catalysis, *Chem. Rev.*, 2020, **120**, 12044–12088.

44 H. L. Tierney, A. E. Baber, J. R. Kitchin and E. C. H. Sykes, Hydrogen dissociation and spillover on individual isolated palladium atoms, *Phys. Rev. Lett.*, 2009, **103**, 246102.

45 G. Kyriakou, M. B. Boucher, A. D. Jewell, E. A. Lewis, T. J. Lawton, A. E. Baber, H. L. Tierney, M. Flytzani-stephanopoulos and E. C. H. Sykes, Isolated Metal Atom Geometries as a Strategy for Selective Heterogeneous Hydrogenations, *Science.*, 2012, **335**, 1209–1213.

46 A. E. Baber, H. L. Tierney, T. J. Lawton and E. C. H. Sykes, An atomic-scale view of palladium alloys and their ability to dissociate molecular hydrogen, *ChemCatChem*, 2011, **3**, 607–614.

47 W. Osada, S. Tanaka, K. Mukai, M. Kawamura, Y. H. Choi, F. Ozaki, T. Ozaki and J. Yoshinobu, Elucidation of the atomic-scale processes of dissociative adsorption and spillover of hydrogen on the single atom alloy catalyst Pd/Cu(111), *Phys. Chem. Chem. Phys.*, 2022, **24**, 21705–21713.

48 H. L. Tierney, A. E. Baber and E. C. H. Sykes, Atomic-scale imaging and electronic structure determination of catalytic sites on Pd/Cu near surface alloys, *J. Phys. Chem. C*, 2009, **113**, 7246–7250.

49 M. D. Marcinkowski, J. Liu, C. J. Murphy, M. L. Liriano, N. A. Wasio, F. R. Lucci, M. Flytzani-Stephanopoulos and E. C. H. Sykes, Selective Formic Acid Dehydrogenation on Pt-Cu Single-Atom Alloys, *ACS Catal.*, 2017, **7**, 413–420.

50 A. Toyoshima, T. Kikuchi, H. Tanaka, K. Mase, K. Amemiya and K. Ozawa, Performance of PF BL-13A, a vacuum ultraviolet and soft X-ray undulator beamline for studying organic thin films adsorbed on surfaces, *J. Phys. Conf. Ser.*, 2013, **425**, 1-4.

51 R. Raval, S. F. Parker and M. A. Chesters, C-H ··· M interactions and orientational changes of cyclohexane on Cu(111): a RAIRS, EELS and LEED study, *Surf. Sci.*, 1993, **289**, 227–236.

52 I. M. Band, Y. I. Kharitonov and M. B. Trzhaskovskaya, Photoionization cross sections and photoelectron angular distributions for x-ray line energies in the range 0.132-4.509 keV Targets: $1 \leqslant Z \leqslant 100$, *At. Data Nucl. Data Tables*, 1979, **23**, 443–505.

53 J. J. Yeh and I. Lindau, Atomic subshell photoionization cross sections and aymmetry parameters: $1 \leqslant Z \leqslant 103$, *At. Data Nucl. Data Tables*, 1985, **32**, 1–155.

54 W. Klaus, Ed., *Surface and Interface Science Volume 1: Concepts and Methods*, Wiley-VCH, 2012.

55 C. S. Hemminger, T. A. Land, A. Christie and J. C. Hemminger, An empirical electron spectrometer transmission function for applications in quantitative XPS, *Surf. Interface Anal.*, 1990, **15**, 323–327.

56 K. Berresheim, M. Mattern-Klosson and M. Wilmers, A standard form of spectra for quantitative ESCA-analysis, *Fresenius. J. Anal. Chem.*, 1991, **341**, 121–124.

57 The code, OpenMX, pseudoatomic basis functions, and pseudopotentials are available at http://www.openmx-square.org.

58 T. Ozaki and H. Kino, Efficient projector expansion for the ab initio LCAO method, *Phys. Rev. B - Condens. Matter Mater. Phys.*, 2005, **72**, 045121.

59 J. P. Perdew, K. Burke and M. Ernzerhof, Generalized gradient approximation made simple, *Phys. Rev. Lett.*, 1996, **77**, 3865–3868.

60 S. Grimme, S. Ehrlich and L. Goerigk, Effect of the damping function in dispersion corrected density functional theory, *J. Comput. Chem.*, 2011, **32**, 1456–1465.

61 S. Grimme, J. Antony, S. Ehrlich and H. Krieg, A consistent and accurate ab initio parametrization of density functional dispersion correction (DFT-D) for the 94 elements H-Pu, *J. Chem. Phys.*, 2010, **132**, 154104.

62 Database (2019) of optimized VPS and PAO for core level excitations, https://t-ozaki.issp.u-tokyo.ac.jp/vps_pao_core2019/.

63 T. Ozaki and C. C. Lee, Absolute Binding Energies of Core Levels in Solids from First Principles, *Phys. Rev. Lett.*, 2017, **118**, 026401.

64 Database (2019) of optimized VPS and PAO, https://t-ozaki.issp.u-tokyo.ac.jp/vps_pao2019/.

65 A. Bach Aaen, E. Lægsgaard, A. V. Ruban and I. Stensgaard, Submonolayer growth of Pd on Cu(111) studied by scanning tunneling microscopy, *Surf. Sci.*, 1998, **408**, 43–56.

66 J. Tang, S. Yamamoto, T. Koitaya, A. Yoshigoe, T. Tokunaga, K. Mukai, I. Matsuda and J. Yoshinobu, Mass transport in the PdCu phase structures during hydrogen adsorption and absorption studied by XPS under hydrogen atmosphere, *Appl. Surf. Sci.*, 2019, **480**, 419–426.

67 M. D. Marcinkowski, A. D. Jewell, M. Stamatakis, M. B. Boucher, E. A. Lewis, C. J. Murphy, G. Kyriakou and E. C. H. Sykes, Controlling a spillover pathway with the molecular cork effect, *Nat. Mater.*, 2013, **12**, 523–528.

68 M. B. Boucher, B. Zugic, G. Cladaras, J. Kammert, M. D. Marcinkowski, T. J. Lawton, E. C. H. Sykes and M. Flytzani-Stephanopoulos, Single atom alloy surface analogs in $Pd_{0.18}Cu_{15}$ nanoparticles for selective hydrogenation reactions, *Phys. Chem. Chem. Phys.*, 2013, **15**, 12187–12196.

69 M. Bowker, R. Holroyd and N. Perkins, The Catalytic Reactivity of Alloys; Ethanol and Formic Acid Decomposition on Cu-Pd(110), *J. Phys. Chem. C*, 2022, **126**, 15703–15709.

70 M. J. Gladys, A. A. El Zein, A. Mikkelsen, J. N. Andersen and G. Held, Chemical composition and reactivity of water on clean and oxygen-covered Pd{111}, *Surf. Sci.*, 2008, **602**, 3540–3549.

71 J. L. Davis and M. A. Barteau, Reactions of carboxylic acids on the Pd(111)-(2 × 2)O surface: multiple roles of surface oxygen atoms, *Surf. Sci.*, 1991, **256**, 50–66.

72 K. K. Rao, Q. K. Do, K. Pham, D. Maiti and L. C. Grabow, Extendable Machine Learning Model for the Stability of Single Atom Alloys, *Top. Catal.*, 2020, **63**, 728–741.

73 M. T. Darby, E. C. H. Sykes, A. Michaelides and M. Stamatakis, Carbon Monoxide Poisoning Resistance and Structural Stability of Single Atom Alloys, *Top. Catal.*, 2018, **61**, 428–438.

74 C. M. Kruppe, J. D. Krooswyk and M. Trenary, Polarization-Dependent Infrared Spectroscopy of Adsorbed Carbon Monoxide to Probe the Surface of a Pd/Cu(111) Single-Atom Alloy, *J. Phys. Chem. C*, 2017, **121**, 9361–9369.

75 S. Surnev, M. Sock, M. G. Ramsey, P. P. Netzer, M. Wiklund, M. Borg and J. N. Andersen, CO adsorption on Pd(111): A high-resolution core level photoemission and electron energy loss spectroscopy study, *Surf. Sci.*, 2000, **470**, 171–185.

76 S. Li, J. Scaranto and M. Mavrikakis, On the Structure Sensitivity of Formic Acid Decomposition on Cu Catalysts, *Top. Catal.*, 2016, **59**, 1580–1588.

77 B. W. J. Chen and M. Mavrikakis, Formic Acid: A Hydrogen-Bonding Cocatalyst for Formate Decomposition, *ACS Catal.*, 2020, **10**, 10812–10825.

78 F. Meng, M. Yang, Z. Li and R. Zhang, HCOOH dissociation over the Pd-decorated Cu bimetallic catalyst: The role of the Pd ensemble in determining the selectivity and activity, *Appl. Surf. Sci.*, 2020, **511**, 145554.

Data for this article, including XPS spectra and outputs of DFT calculations are available at ScienceDB at https://doi.org/10.57760/sciencedb.14315.